

Direct Electrochemistry of Myoglobin and Cytochrome P450_{cam} in Alternate Layer-by-Layer Films with DNA and Other Polyions

Yuri M. Lvov,^{*,†} Zhongqing Lu,[†] John B. Schenkman,[‡] Xiaolin Zu,[†] and James F. Rusling^{*,†}

Contribution from the Chemistry Department, U-60, University of Connecticut, Storrs, Connecticut 06269-4060, and Department of Pharmacology, University of Connecticut Health Center, Farmington, Connecticut 06032

Received November 4, 1997

Abstract: Alternate layer-by-layer polyion adsorption onto gold electrodes coated with chemisorbed mercapto-propanesulfonic acid gave stable, electroactive multilayer films containing the proteins myoglobin and cytochrome P450_{cam}. Direct, reversible, electron exchange between gold electrodes and proteins involved heme Fe^{III}/Fe^{II} redox couples. With oxygen in solution, electrons were also transferred to the Fe^{II}-O₂ complexes of these proteins, a key step for oxidative enzyme catalysis. Film assembly for Mb was done by sequential adsorption with poly(styrenesulfonate) (PSS), DNA, or poly(dimethyl diallyl) ammonium chloride (PDDA). Cyt P450_{cam} was assembled with layers of PSS or PDDA. Quartz crystal microbalance and voltammetric studies on the same films allowed quantitation of electroactive and nonelectroactive protein. At pH 5.5, the first protein monolayer in all films was fully electroactive. A second monolayer added 30–40% redox activity, but additional protein layers did not communicate with the electrode. Using various film construction strategies, Mb monolayers were also placed at distances from the electrodes of 0.5, 1.8, and 3.8 nm. Full electroactivity was found at 0.5 nm, and about 70–80% electroactivity at 1.8 and 3.8 nm. Results suggest the possibility of enhanced electron transport by partial intermixing of protein and nonprotein layers. Polyion films containing Mb and cyt P450_{cam} were active for enzyme-like catalysis of styrene epoxidation in aerobic solutions.

Introduction

Reversible redox transformations of enzymes at electrodes can be used to drive enzyme-catalyzed reactions.¹ Enzyme-coated electrodes provide a basis for biosensors, biomedical devices, and enzymatic bioreactors.² Achieving direct electron exchange between electrodes and enzymes simplifies these devices by removing the requirement for a chemical mediator.

Long-term goals of our research include development of electrode coatings for studies of toxic activation of pollutants, which is often catalyzed by the iron heme enzymes cytochrome P450 (cyt P450) in the liver.³ Pollutants activated by enzyme-catalyzed oxidation can damage DNA, possibly causing disease. An initial electron transfer to cyt P450Fe^{III} begins the catalytic cycle for oxidation of lipophilic pollutants and drugs.⁴ Thus,

it is essential to achieve this key reduction on an electrode if applications of electrochemically driven enzyme catalysis with cyt P450 are to succeed.

We recently reported the direct reversible voltammetry of the heme Fe(III)/Fe(II) redox couple of bacterial cyt P450_{cam} in thin films of dimyristoylphosphatidylcholine (DMPC) and didodecyltrimethylammonium bromide (DDAB) on pyrolytic graphite (PG) electrodes.⁵ Films were prepared by a casting method, first developed using the iron heme protein myoglobin.⁶ These films supported enzyme-like reductive electrochemical catalysis of organohalide pollutants.⁷

An important feature of the protein-surfactant films is that they can “turn on” protein electron-transfer reactions. Thus, while reversible voltammetry of Mb or cyt P450_{cam} can be

[†] University of Connecticut.

[‡] University of Connecticut Health Center.

(1) (a) Armstrong, F. A.; Hill, H. A. O.; Walton, N. J. *Acc. Chem. Res.* **1988**, *21*, 407–413. (b) Armstrong, F. A. In *Bioinorganic Chemistry, Structure and Bonding* 72; Springer-Verlag: Berlin, 1990; pp 137–221. (c) Heller, A. *Acc. Chem. Res.* **1990**, *23*, 128–134. (d) Bourdillon, C.; Demaille, C.; Moiroux, J.; Saveant, J. M. *Acc. Chem. Res.* **1996**, *35*, 529–535.

(2) For examples, see: (a) Wilson, G. In *Biosensors*; Turner, A., Karube, I., Wilson, G., Eds.; Oxford University Press: New York, 1987. (b) Chaplin, M. F.; Bucke, C. *Enzyme Technology*; Cambridge University Press: U.K., 1990. (c) Kauffmann, J. M.; Guilbault, G. G. In *Bioanalytical Applications of Enzymes, Methods Biochem. Anal.*; Wiley: New York, 1992; Vol. 36, pp 63–113.

(3) (a) *Enzymatic Basis of Detoxification*; Jacoby, W. B., Ed.; Academic: New York, 1980; Vols. I and II (b) Singer, B.; Grunberger, D. *Molecular Biology of Mutagens and Carcinogens*, Plenum: New York, 1983.

(4) (a) Guengerich, F. P.; MacDonald, T. L. *Acc. Chem. Res.* **1984**, *17*, 9–16. (b) *Cytochrome P450*, 2nd ed.; Ortiz de Montellano, P. R., Ed.; Plenum: New York, 1995. (c) *Cytochrome P450*; Schenkman, J. B., Greim, H., Eds.; Springer-Verlag: Berlin, 1993. (d) *Cytochrome P450*, 2nd ed.; Omura, T.; Ishimura, Y.; Fujii-Kuriyama, Y., Eds.; Kodansha/VCH: Tokyo, 1993.

(5) Zhang, Z.; Nassar, A.-E. F.; Lu, Z.; Schenkman, J. B.; Rusling, J. F. *J. Chem. Soc., Faraday Trans.* **1997**, *93*, 1769–1774.

(6) (a) Rusling, J. F.; Nassar, A.-E. *J. Am. Chem. Soc.*, **1993**, *115*, 11891–11897. (b) Rusling, J. F. *Prog. Colloid Polymer Sci.* **1997**, *103*, 170–180. (c) Nassar, A.-E. F.; Narikiyo, Y.; Sagara, T.; Nakashima, T.; Rusling, J. F. *J. Chem. Soc., Faraday Trans.* **1995**, *91*, 1775–1782. (d) Nassar, A.-E.; Willis, W.; Rusling, J. F. *Anal. Chem.* **1995**, *67*, 2386–2392. (e) Zhang, Z.; Rusling, J. F. *Biophys. Chem.* **1997**, *63*, 133–146. (f) Nassar, A.-E. F.; Zhang, Z.; Hu, N.; Rusling, J. F.; Kumosinski, T. *J. Phys. Chem.* **1997**, *101*, 2224–2231. (g) Nassar, A.-E. F.; Rusling, J. F.; Kumosinski, T. F. *Biophysical Chem.* **1997**, *67*, 107–116.

(7) Nassar, A.-E.; Bobbitt, J.; J. D. Stuart, J.; Rusling, J. *J. Am. Chem. Soc.* **1995**, *117*, 10986–10993.

obtained in films of insoluble surfactants,^{5–7} direct electron transfer between bare pyrolytic graphite (PG) electrodes and cyt P450_{cam} in solution was observed only at the edge plane at low temperature in highly purified solutions.⁸ Similarly, electron transfer between myoglobin (Mb) in solution and bare electrodes is slow except in highly purified solutions with specially prepared “hydrophilic” indium tin oxide electrodes.⁹ On PG, Au or Pt electrodes, electrochemistry of Mb or cyt P450_{cam} is not observable under conditions which yield reversible voltammetry in DDAB or DMPC films.^{5,6}

Films cast from vesicles or solutions of DDAB, DMPC, and other insoluble surfactants self-assemble with surfactant molecules organized into stacks of bilayers.^{6a,b,c,e,10} These films are quite useful for electrochemical applications of proteins, but their structures are governed by molecular properties and interactions which guide the self-assembly process. The final architecture of these films is not under the control of the experimentalist.

The principle of alternate adsorption can be used to design specific film architectures. It was invented for oppositely charged colloidal particles in the pioneering work of Iler.¹¹ Later, it was adapted for polymer films by means of alternate adsorption of polycations and polyanions^{12–14} The approach is related to Mallouk’s concept of multilayer synthesis based on sequential adsorption of Zr⁴⁺ ions and diphosphonic acid.¹⁵

Studies described in this paper were aimed at exploring applications of alternate polyion adsorption to protein electrochemistry. The standard procedure is illustrated as follows: A solid substrate with positively charged planar surface is immersed in a solution of anionic polyelectrolyte, and a layer of polyanion is adsorbed. The adsorption is done at relatively high concentration of polyelectrolyte, and a number of ionic groups remain exposed at the interface with the solution. Thus, the surface charge is effectively reversed. After rinsing in pure water, the substrate is immersed in a solution of cationic polyions. A new layer is adsorbed, but now the original positive surface charge has been restored. By repeating both steps, alternating multilayer assemblies are obtained. The polyions may be linear or globular, like soluble proteins. Naturally, polyions have to be adsorbed at a solution pH that provides a high degree of ionization. In this method the crucial feature is excessive adsorption, i.e., in excess of neutralization, that leads to recharging of the outermost surface at every step of film formation.

This technique was recently applied to many water soluble polyions, including DNA.^{12,13} It has been used for charged particles, ceramics, gold nanoparticles, and proteins.^{14–18} Protein-polyion multilayer assembly opens the possibility of organizing

proteins in layers designed following specific molecular architectural plans.^{17,18} Electrochemical studies of polyion multilayers containing poly(oxometalate),¹⁹ poly(butyl viologen)/poly(styrenesulfonate),²⁰ ferrocyanide/poly(vinylmethylpyridinium),²¹ and glucose oxidase/poly(allylamine)ferrocene²² were recently described. In a related approach, Bowden and co-workers attached alkylthiol monolayers terminating in carboxylate groups to gold and obtained reversible electron transfer to positively charged, adsorbed cytochrome *c*.^{23a} Carboxylthiol-Au was also used to adsorb successive layers of positively charged poly(lysine) and negatively charged cytochrome b5 and achieve reversible electrochemistry.^{23b} Electrochemistry of protein *multilayers* in alternate polyion films has not been reported previously, to our knowledge.

In this paper, we explore polyion layer-by-layer adsorption for preparing multilayer electroactive films of redox proteins. We describe ultrathin (5–10 nm) films on gold electrodes of myoglobin (Mb) or cytochrome P450_{cam} (cyt P450_{cam}) assembled layer-by-layer with oppositely charged polyions, including DNA, acting as “electrostatic glue”. Mb and cyt P450_{cam} in these films both gave direct reversible heme Fe^{III}/Fe^{II} electrochemistry from the proteins in layers closest to the electrode. The protein films catalyzed electrode-driven aerobic oxidation of styrene.

Experimental Section

1. Materials. *Pseudomonas putida* cytochrome P450_{cam} (MW 46 500) was obtained and purified as described previously.^{5,24a} Horse heart myoglobin (Mb, Sigma, MW 17 400) solutions were ultrafiltered through a YM30 filter (Amicon, 30 000 MW cutoff).^{6d} Polyions used were sodium poly(styrenesulfonate) (PSS, MW 70 000, Aldrich), poly(dimethyldiallylammonium chloride) (PDDA, Aldrich), branched poly(ethyleneimine) (PEI, MW 70 000, Wako, Japan), and calf thymus double strand (CT-ds) DNA (Sigma).

2. Film Assembly. Multilayer films were assembled on gold-coated quartz crystal microbalance (QCM) resonators or on quartz plates. A negatively charged gold surface was prepared by coating with 3-mercaptopropylsulfonic acid (MPS). No voltammetric peaks were detected in films on gold without MPS coatings.

Films were grown by repeated alternate adsorption from aqueous solutions of proteins, PSS, PDDA, and DNA. In some cases, polyion adsorption was done from salt solutions and denoted with a salt concentration, e.g., PSS (0.1 M NaCl) or PSS (0.5 M NaCl). Solid substrates were alternately immersed for 15 min in aqueous solutions of proteins or polyions with intermediate washing with water. Films were dried under a stream of nitrogen for QCM or visible spectroscopy.

3. Quartz Crystal Microbalance Studies. QCM (USI System, Japan) measurements were used to monitor film growth: (i) after each adsorption step, the resonator was immersed in polyelectrolyte solution for a given period, dried with nitrogen, and the frequency change

(8) Kazlauskaitė, J.; Westlake, A.; Wong, L.-L.; Hill, H. *J. Chem. Soc., Chem. Commun.* **1996**, 2189–2190.

(9) (a) Taniguchi, I.; Watanabe, K.; Tominaga, M.; Hawkrigde, F. M. *J. Electroanal. Chem.* **1992**, 333, 331–388. (b) Taniguchi, I.; Kurihara, H.; Yoshida, K.; Tominaga, M.; Hawkrigde, F. *Denki Kagaku* **1992**, 60, 1043–1049.

(10) Nassar, A.-E. F.; Zhang, Z.; Rusling, J. F.; Chynwat, V.; Frank, H. A.; Suga, K. *J. Phys. Chem.* **1995**, 99, 11013–11017.

(11) Iler, R. *J. Colloid and Interface Sci.* **1966**, 21, 569–594.

(12) (a) Decher, G.; Hong, J.-D. *Ber. Bunsen-Ges. Phys. Chem.* **1991**, 95, 1430–1434. (b) Lvov, Y.; Decher, G.; Möhwald, H. *Langmuir* **1993**, 9, 481–486. (c) Lvov, Y.; Decher, G.; Sukhorukov, G. *Macromolecules* **1993**, 26, 5396–5399.

(13) (a) Ferreira, M.; Rubner, M. *Macromolecules* **1995**, 28, 7107–7114. (b) Hammond, P.; Whitesides, G. *Macromolecules* **1995**, 28, 7569–7571.

(14) (a) Kleinfeld, E.; Ferguson, G. *Science* **1994**, 265, 370–373. (b) Fendler, J.; Meldrum, F. *Adv. Mater.* **1995**, 7, 607–632. (c) Decher, G. *Science* **1997**, 227, 1232–1237.

(15) (a) Lee, H.; Kepley, L.; Hong, H.-G.; Mallouk, T. *J. Am. Chem. Soc.* **1988**, 110, 618–622. (b) Keller, S.; Kim, H.-N.; Mallouk, T. *J. Am. Chem. Soc.* **1994**, 116, 8817–8818.

(16) (a) Lvov, Y.; Ariga, K.; Kunitake, T. *Chem. Lett.* **1994**, 2323–2326. (b) Kong, W.; Wang, L. P.; Gao, M. L.; Zhou, H.; Zhang, X.; Li, W.; Shen, J. *J. Chem. Soc., Chem. Commun.* **1994**, 1297–1298. (c) Schmitt, J.; Decher, G.; Dressik, W.; Brandow, S.; Geer, R.; Shashidhar, R.; Calvert, J. *Adv. Materials* **1997**, 9, 61–65.

(17) Lvov, Y.; Ariga, K.; Ichinose, I.; Kunitake, T. *J. Am. Chem. Soc.* **1995**, 117, 6117–6123.

(18) Onda, M.; Lvov, Y.; Ariga, K.; Kunitake, T. *J. Ferment. Bioeng.* **1996**, 82, 502–506.

(19) Ingersoll, D.; Kulesza, P.; Faulkner, L. *J. Electrochem. Soc.* **1994**, 141, 140–147.

(20) Laurent, D.; Shlenoff, J. *Langmuir* **1997**, 13, 1552–1556.

(21) Lowy, D.; Finklea, H. *Electrochim. Acta* **1997**, 42, 1325–1335.

(22) Hodak, J.; Etchenique, R.; Calvo, E.; Singhal, K.; Bartlett, P. *Langmuir* **1997**, 13, 2708–2716.

(23) (a) Tarlov, M. J.; Bowden, E. F. *J. Am. Chem. Soc.* **1991**, 113, 1847–1849. (b) Glenn, J. D. H.; Bowden, E. F. *Chem. Lett.* **1996**, 399–400.

(24) (a) O’Keefe, D.; Ebel, R.; Peterson, J. *Methods Enzymol.* **1978**, 52, 151–157. (b) Sauerbrey, G. *Z. Physik* **1959**, 155, 206–214. (c) Zhang, Z.; Zu, X.; Lu, Z.; Schenkman, J. B.; Rusling, J. F. *Biochem. Biophys. Res. Comm.* In press.

measured, and (ii) for *in-situ* monitoring of adsorption, only one side of the resonator was placed in contact with the surface of the solution and the frequency change was recorded continuously. The quartz resonators (USI Systems, Fukuoka, Japan) were covered by gold electrodes on both faces and their resonance frequency was 9 MHz (AT-cut). The surface roughness factor of these electrodes was previously estimated¹⁷ at 1.1 ($\pm 5\%$) by scanning electron microscopy. Reproducibility was ± 2 Hz over 2 h.

We estimated the mass increase [M (g)] for adsorption from the QCM frequency shift [ΔF (Hz)] of dry films by using the Sauerbrey equation.^{24b} Taking into account resonator characteristics, the following relation obtains

$$\Delta F = -1.83 \times 10^8 M/A \quad (1)$$

where $A = 0.16 \pm 0.01$ cm², the apparent area of the microbalance electrodes. The thickness (d) of film on both sides of the electrode was estimated as described previously, from¹⁷

$$d \text{ (nm)} \approx -0.016 \Delta F \text{ (Hz)} \quad (2)$$

4. Electrochemistry. A BAS-100B/W electrochemical analyzer was used for cyclic voltammetry (CV) and controlled-potential electrolysis. The three-electrode cell contained the coated gold QCM working electrode, a platinum wire counter electrode, and a saturated calomel reference electrode (SCE). Ohmic drop of the cell was 98–99% compensated by the BAS-100B/W. Prior to CV, solutions were purged with purified nitrogen. When needed, pure oxygen was purged through solutions. CV measurements were done at 22–23 °C. Uncompensated resistance and capacitance were estimated by using the Auto iR Comp function of the BAS-100B/W.

5. Catalytic Activity. Films used for catalytic oxidation of styrene were made on both sides of 1.5 × 4 cm gold foil (Aldrich) electrodes, using methods described above. Electrolyses were done at –0.6 V vs SCE with oxygen passing through the solution. After 1 h, samples were extracted with CH₂Cl₂ and analyzed by gas chromatography.^{24c}

Results

1. Assembly of Myoglobin/Polyanion Multilayers. Mb layers were adsorbed from pH 5 buffer, where Mb has a surface charge²⁵ of +7. Films of cationic myoglobin and negatively charged PSS or DNA (Mb/PSS or Mb/DNA multilayers) were assembled on negative MPS-gold or quartz surfaces by alternate 15 min adsorption. QCM monitoring of the assembly process showed linear change of the frequency with cycles of adsorption (Figure 1a) for both assemblies. This indicates a linear increase of film mass with increasing number of layers.

Film mass and thickness estimates based on eqs 1 and 2 were verified previously¹⁷ by directly calibrating dry film frequency shifts on the same types of resonators used in the present work with protein/polyion film thickness from scanning electron microscopy of cross-sections. We estimated mass and thickness only for dry films.

For every layer of Mb adsorption, QCM frequency (F) decreased 300 Hz. After each DNA adsorption step, F decreased 130 Hz. These changes correspond to film mass increases of 840 ng cm⁻² for Mb layers and 370 ng cm⁻² for DNA layers, respectively. These masses correspond to a 4.8 nm thickness for each Mb layer and 2.0 nm for each DNA layer. Taking into account crystallographic dimensions^{26a} of Mb 2.5 × 3.5 × 4.5 nm and double-stranded DNA diameter of 1.9 nm,^{12c} we conclude that monomolecular layers form at every step of the assembly process. The first Mb layer had a slightly smaller

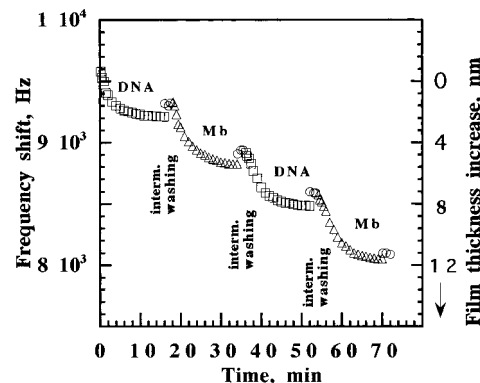
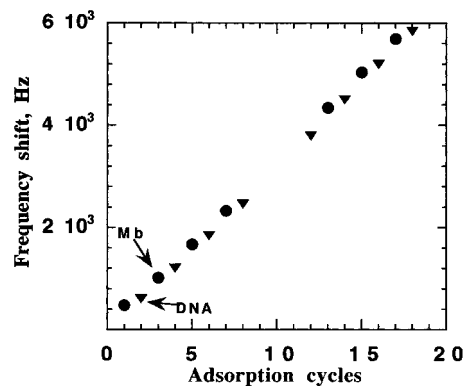


Figure 1. QCM monitoring of (a) linear growth for dried Mb/DNA multilayers films at pH 5. Steps 8–11 are assembled without interrupting the process for drying, and (b) *in situ* kinetics of Mb/DNA sequential assembly, both on Au-MPS-Mb underlayer.

thickness, $-\Delta F = 200$ Hz, corresponding to 560 ng cm⁻² and 3.2 nm thickness.

In-situ QCM in solution was used only for observing adsorption kinetics to establish the time for adsorption saturation. Figure 1b shows *in-situ* QCM measurements of kinetics of alternate DNA/Mb adsorption. In the first step, DNA was adsorbed onto an underlying layer of Mb on MPS–Au. The QCM frequency decreases sharply because of rapid adsorption during the first 10 min, after which a slower change is observed as adsorption saturation sets in.

Following each saturation adsorption step, the resonator was rinsed in pure water. Measurements taken immediately after rinsing are denoted by the open circles in Figure 1b. The frequency after rinsing increased about 20% of the total frequency shift observed in the previous adsorption step and then remained constant. This suggests that in pure water about 20% of the adsorbed DNA was removed, presumably involving weakly attached molecules.^{26b} After washing, the film was immersed in a Mb solution and Mb adsorption proceeded, reaching saturation in 12 min. Then once more, the resonator was immersed in pure water. Frequency increased 20% after washing, reflecting removal of part of the Mb. Subsequently, in the third step, the film was immersed in DNA solution. This stage of DNA adsorption is similar to the first step (Figure 1b). Then the film was washed in water, and placed in Mb solution once more. Each subsequent step was quite reproducible, and adsorption always reached saturation. A 15 min adsorption period provided saturation at every cycle.

(26) (a) Kendrew, J.; Phillips, D.; Stone, V. *Nature* **1960**, *185*, 422–429. (b) It is unlikely that small viscosity differences between water and polyelectrolyte solutions influence QCM frequencies significantly. Nearly identical QCM frequencies in water after film washing and in the subsequent polyelectrolyte solutions (cf. Figure 1b) at the very beginning of an adsorption step support this view.

(25) (a) Shire, S. J.; Hanania, G. I. H.; Gurd, F. R. N. *Biochemistry* **1974**, *13*, 2967–2980. (b) Friend, S. H.; Gurd, F. R. N. *Biochemistry* **1979**, *18*, 8, 4612–4619.

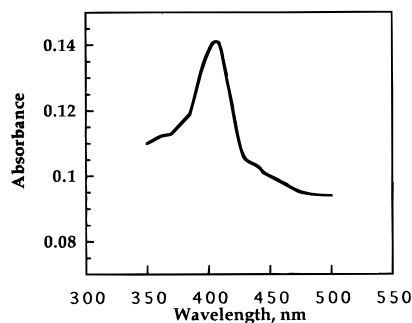


Figure 2. Visible absorbance spectrum of $(\text{Mb/PSS})_8$ multilayer film on quartz.

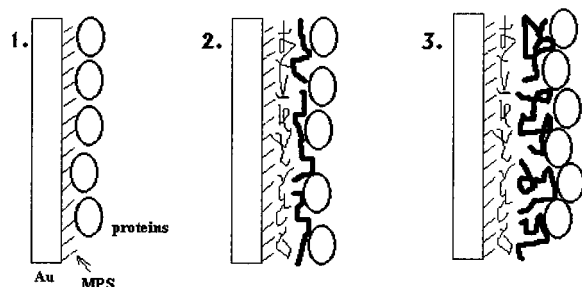


Figure 3. Conceptual picture of different film architectures with Mb located 1. 0.5 nm above Au on MPS monolayer, 2. 1.8 nm above Au on layer of {MPS + PEI/PSS}, and 3. 3.8 nm above Au on layer {MPS + PEI/PSS (0.5 M NaCl)}.

Similar kinetics were obtained for alternate Mb/PSS adsorption, and the film showed linear QCM frequency changes as in Figure 1a. Steps of multilayer growth as monitored by QCM were $-\Delta F = 350$ Hz, or 980 ng cm^{-2} for Mb and $-\Delta F = 50$ Hz or 140 ng cm^{-2} for PSS. The very first Mb layer in the film was thinner, with $-\Delta F = 200$ Hz or 560 ng cm^{-2} . Similar to the assembly of Mb/DNA, monolayers of the protein were formed at every other deposition step.

Figure 2 shows UV-spectra of Mb/PSS (0.1 M NaCl) multilayers. The heme Soret band at 402 nm is slightly smaller than the 408 nm observed in neutral solution.²⁷ This suggests that the Mb may be partly unfolded in the film or that the polymeric medium influences the iron heme environment and thereby the Soret band frequency.

Salt in the adsorbate solutions neutralizes polyions, induces coiling,^{12a,b} and thickens the adsorbed layer. Thus, layer thickness of PSS adsorbed from water is ca. 0.8 nm, but adsorption from 0.5 M NaCl solution gives 3 nm layers. We calculated these values from the corresponding QCM frequency shifts of 50 and 180 Hz, respectively. Subsequently, we found that more Mb is deposited on the thicker layer of PSS.

Using salt to vary polyion layer thickness, we prepared three films for electrochemical study in which the Mb layer was grown at different distances from the electrode surface (Figure 3):

(1) A Mb monolayer of $560 \text{ ng cm}^{-2} = 0.32 \times 10^{-10} \text{ mol cm}^{-2}$ was deposited onto an MPS-gold electrode. The MPS monolayer thickness is 0.5 nm, calculated from $-\Delta F = 30$ Hz.

(2) A PEI/PSS bilayer was assembled on MPS-gold with thickness of 1.3 nm, on top of which a Mb layer of $980 \text{ ng cm}^{-2} = 0.57 \times 10^{-10} \text{ mol cm}^{-2}$ was deposited.

(3) A thicker PEI/PSS (0.5 M NaCl) layer of 3.3 nm was assembled on MPS-gold, on top of which a Mb layer of $1690 \text{ ng cm}^{-2} = 0.96 \times 10^{-10} \text{ mol cm}^{-2}$ was deposited.

Based only on QCM, we cannot state that the Mb layers are precisely at the estimated distances. We do not exclude that

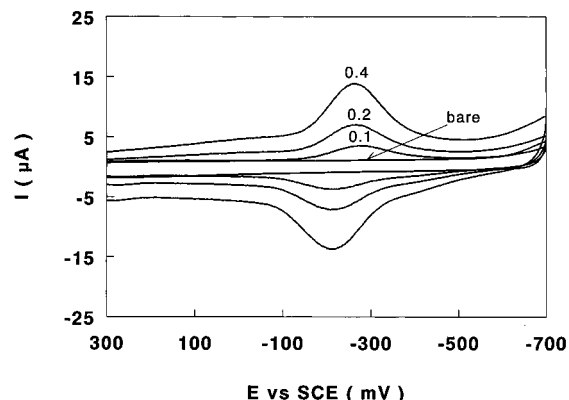
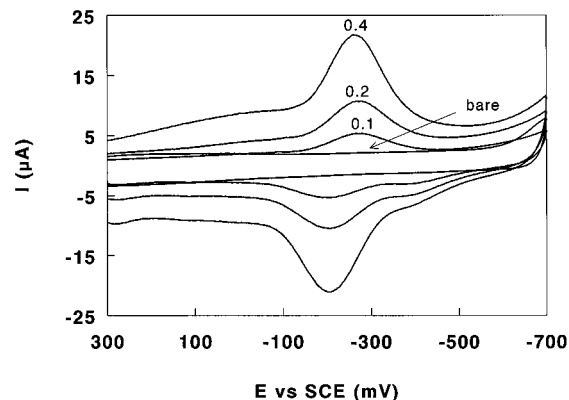


Figure 4. Cyclic voltammograms in 0.1 M KCl, 0.1 M acetate buffer, pH 5.5 of (a) Mb monolayer on Au-MPS and (b) Mb/PSS bilayer on Au-MPS. Scan rates 0.1, 0.2, and 0.4 V s^{-1} marked on curves, with curve marked "bare" for Au + {MPS + PEI/PSS} electrode.

the Mb globules partially sink into PSS layers. This may in fact be reasonable, since we find that larger amounts of Mb are attached to the thicker PEI/PSS underlayers.

2. Voltammetry of Mb Monolayers and Mb/PSS Bilayers.

In all experiments with Mb and Mb/PSS films in anaerobic solutions, a total of 12 samples, we found reversible, reproducible $\text{MbFe}^{\text{III}}/\text{MbFe}^{\text{II}}$ peaks by cyclic voltammetry. After a film was prepared, we immersed it into a buffer solution and scanned the potential between 0.3 and -0.7 V vs SCE continuously at 0.1 V s^{-1} for 2 min, after which the voltammetric signals remained stable. We did not observe reductive desorption of the alkylthiol monolayer from gold in this potential range as was reported at -0.74 V earlier.²⁸

Figure 4 shows cyclic voltammograms (CV) for a Mb monolayer and a Mb/PSS bilayer on MPS-Au. Reversible pairs of reduction-oxidation peaks were observed with an average midpoint potential at pH 5.5 of -0.235 V vs SCE (0.007 V vs NHE). The shapes of these peaks are nearly symmetric, with equal reduction and oxidation peak heights. Plots of log peak current vs log scan rate (up to 1 V s^{-1}) had correlation coefficients of 0.999 with slopes of 1.005, close to the theoretical slope of 1 for thin layer voltammetry.²⁹ These results suggest that all of the electroactive MbFe^{III} in the film is converted to MbFe^{II} on the forward scan to negative potentials, with full conversion of MbFe^{II} to MbFe^{III} on the reversed scan.

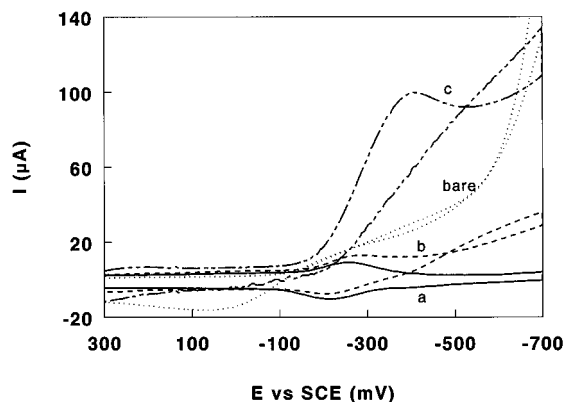
From QCM, the amount of Mb on the electrode is $560 \pm 50 \text{ ng cm}^{-2}$ ($0.32 \times 10^{-10} \text{ mol cm}^{-2}$, Table 1). The integral under

(27) (a) Theorell, H.; Ehrenberg, A. *Acta Chem. Scand.* **1951**, *5*, 823–848. (b) George, P.; Hanania, G. *Biochem. J.* **1952**, *52*, 517–523. (c) Herskovits, T. T.; Jailliet, H. *Science* **1969**, *163*, 282–285.

(28) Imabayashi, S.; Hobar, D.; Kakiuchi, T.; Knoll, W. *Langmuir* **1997**, *13*, 4502–4504.

Table 1. Mb/PSS (0.1 M NaCl) Multilayers on MPS-Treated Gold Electrode CV Measurements Performed at pH 5.5 in 0.1 M KCl

film composition	E° V vs NHE	CV charge $\mu\text{C cm}^{-2}$	10^{10} mol cm^{-2} Mb	
			electroactive	QCM
Mb	0.007	3.4	0.36	0.32
Mb/PSS	0.002	2.8	0.29	0.32
Mb/PSS/Mb	0.007	3.8	0.40	0.64
Mb/PSS/Mb/PSS	0.007	3.2	0.33	0.64

**Figure 5.** Cyclic voltammograms at 0.2 V s^{-1} in 0.1 M KCl pH 5.5 buffer for $(\text{Mb/PSS})_2$ film: (a) under N_2 , (b) after 3 min exposure of solution to air, (c) after bubbling 20 mL O_2 through the electrolyte with cell closed, and “bare” gold electrode after bubbling 20 mL O_2 through the electrolyte.

the reduction peak gives the number of moles of electroactive protein in the thin film.²⁹ Integration of the CVs of Mb monolayers gave an average surface concentration of electroactive Mb in the film of $620 \pm 30 \text{ ng cm}^{-2}$ ($0.36 \cdot 10^{-10} \text{ mol cm}^{-2}$). At pH 5.5, the amounts of total and electroactive protein on the electrode are similar.

The CV peak width of 0.12 V at half-height is larger than the theoretically predicted 0.09 V for ideal surface waves.²⁹ This may result from a distribution of distances and/or orientations of Mb and/or interactions between Mb units in the films. Reduction–oxidation peak separation was 0.05 V for scan rates $0.1\text{--}1 \text{ V s}^{-1}$. Interestingly, after a number of sweeps the cell resistance remained the same (ca. $200 \Omega \text{ cm}^{-2}$), but the capacitance typically doubled. This capacity increase may be connected with redistribution of charge in the film and diffusion of ions from electrolyte into or out of the film.

After deposition of a PSS monolayer on top of the layer of Mb (Figure 4b), the shape, width, and symmetry of the peaks remained the same, but peak current decreased about 25%. The deposition of PSS gives a coverage with thickness of ca. 0.8 nm. One reason for this decrease in charge may be dissolution of some Mb during film immersion in PSS solution.

Mb in the Mb/PSS bilayer is more strongly bound than in the monolayer and may be used for several weeks without significant detachment from the gold electrodes. CV peaks from Mb/PSS bilayers kept for a week in air at room-temperature coincided with the initial peaks within 5–10%.

Reversible CV peak potentials and currents were dependent on solution pH. Formal potentials vs NHE were 0.01 V at pH 5, -0.09 V at pH 7, and -0.20 V at pH 8.6. The shift of the formal potential was $-0.055 \pm 0.005 \text{ V pH}^{-1}$ unit. The largest

Table 2. Mb/DNA (0.01 M NaCl) Multilayers on MPS-Treated Gold Electrode^a

film composition	E° V vs NHE	CV charge $\mu\text{C cm}^{-2}$	10^{10} mol cm^{-2} Mb	
			electroactive	QCM
Mb/DNA	0.014	3.4	0.35	0.32
Mb/DNA/Mb	0.015	3.4	0.35	0.64
Mb/DNA/Mb/DNA	0.007	2.8	0.29	0.64

^a CV measurements performed at pH 5.5 in 0.1 M KCl.

CV peak currents were detected at pH 5. At pH 7, peaks decreased to 60% of values at pH 5 and to 30% at pH 8.6. This tendency is similar to the results for Mb in cast films of didodecyldimethylammonium bromide (DDAB) or phosphatidylcholines.^{6f} QCM before and after electrochemical studies showed that the Mb/PSS multilayer was stable, and there was no mass depletion from the electrodes. Changes in the CVs were reversible. That is, a film that had been removed from the pH 5 solution, and had its CV run in pH 8.6 buffer, gave a CV the same as the original at pH 5 upon returning again to the pH 5 buffer.

3. Influence of Oxygen on CV. We also studied CVs of Mb films in the presence of dissolved oxygen. CVs of $(\text{Mb/PSS})_2$ films under nitrogen atmosphere, after keeping the cell open to air 2 min, and after passing 20 mL of pure oxygen through the electrolyte in a sealed cell are shown in Figure 5. Addition of oxygen caused an increase in current at the potential of the reduction of MbFe^{III} in 0.1 M KCl, 0.1 M acetate buffer, pH 5.5, and disappearance of the anodic peak for the oxidation of MbFe^{II} . Results are consistent with the initial reduction $\text{MbFe}^{\text{III}} \rightarrow \text{MbFe}^{\text{II}}$, reaction of the MbFe^{II} with oxygen, and reduction of the $\text{MbFe}^{\text{II}}\text{--O}_2$ complex to give hydrogen peroxide. This process has been observed in Mb-DDAB films, in microemulsions, and in aqueous buffers^{30a,b} and is discussed in more detail in section 7 below.

4. Electrochemistry of Mb/DNA Multilayers. Mb was adsorbed on an MPS-gold electrode, and then a DNA layer was adsorbed. After CVs were obtained in a buffer solution, and the next layer of Mb and DNA was added. Table 2 summarizes CV and QCM results on these films. After deposition of Mb/DNA, about 5 min of potential sweeping was needed to obtain stable and reproducible CVs (Figure 6). A small transient peak at -0.37 V vs SCE decreased after a few scans, as symmetric reduction/oxidation peaks appeared. CVs of Mb/DNA bilayers are similar to CVs of Mb/PSS bilayers, and no specific features of DNA were observed in the potential range used. Peak current was proportional to scan rate.

5. Myoglobin Multilayers at Different Distances from the Electrode. We built up alternating PSS, DNA, and Mb layers on top of Au-MPS-Mb, and measured CV after every newly deposited layer. Results are summarized in Tables 1–3. There was no linear increase in peak current or integrated charge with increasing number of Mb/PSS layers. Except for films with DNA, a second Mb layer provides increases in charge of 30–40% over Au-MPS-Mb/PSS, but no further increase with additional Mb layers was detected. A periodic change of charge with a number of layers (Tables 1 and 3), featuring a decrease when an outermost polyanion layer is added, may be connected with loss of some protein in the outer layer during immersion

(29) (a) Murray, R. W. In *Electroanalytical Chemistry*; Bard, A. J., Ed.; Vol. 13, Marcel Dekker: New York, 1984; pp 191–368. (b) Murray, R. W. In *Molecular Design of Electrode Surfaces*; Murray, R. W., Ed.; John Wiley & Sons: New York, 1992; pp 1–48.

(30) (a) Onuoha, A.; Rusling, J. F. *Langmuir* **1995**, *11*, 3296–3301. (b) Onuoha, A.; Zu, X.; Rusling, J. F. *J. Am. Chem. Soc.* **1997**, *119*, 3979–3986. (c) Immersion of a Au-MPS-PEI/PSS electrode in 0.2 mg mL^{-1} ferroheme in pH 9.8 buffer gave no increase in weight by QCM and only a 2% difference in current by CV before and after immersion, with no peaks observed. This suggests that ferroheme would not remain in PSS/protein films if released from the protein.

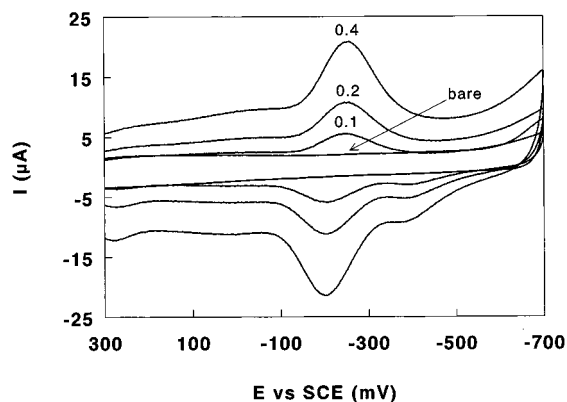


Figure 6. Cyclic voltammograms in 0.1 M KCl pH 5.5 buffer at scan rates of 0.1, 0.2, and 0.4 V s⁻¹ for Mb/DNA bilayer on Au-MPS, curve marked "bare" is for Au + {MPS + PEI/PSS} electrode.

in polyanion solution. The Mb monolayer closest to the electrode gave the main fraction of CV charge.

Films with single Mb monolayers with different average Mb-to-Au distances gave similar voltammograms. The Mb monolayer is located about 0.5 nm from the Au surface in the Au-MPS-Mb system, and we find a ratio of about 1.1:1 of moles electroactive Mb to total moles of Mb measured by QCM (Table 1). In the Au-MPS-PEI/PSS/Mb system, Mb is 1.8 nm away from the gold surface, and the electroactive:total molar ratio is 0.7:1. In the Au-MPS-PEI/PSS (0.5 M NaCl)/Mb film the Mb-Au separation is 3.8 nm, and the electroactive:total molar ratio is 0.8:1. Thus, a large fraction of the Mb in all of these layers is electroactive.

It is not clear why the charge for the Mb layer deposited directly on MPS-treated electrode is slightly higher than the corresponding mass. Certainly this could result from errors in the integrated charge. It is unlikely that partial denaturation of Mb results in increased free ferroheme at the electrode surface. Free ferroheme placed into cast DDAB films was leached out within several CV scans,^{6d} and we might expect a similar observation if ferroheme was free in the layered polyanion films. This is not the case, as the CV signals for all films are stable for up to a week. Furthermore, the ferroheme contains two propionic acid groups^{25b} with $pK_a \approx 4$ which would be largely ionized at pH 5 and would be repelled from the negative MPS-Au surface.^{30c}

In both Au-MPS-PEI/PSS/Mb and Au-MPS-PEI/PSS (0.5 M NaCl)/Mb films, Mb is located on a soft polyanion layer, and the majority of the protein is electroactive. The separating layer is a PEI/PSS bilayer, in which Mb globules could be partially sunk. Also, we do not exclude partial penetration of Mb through the polyanion layer to the electrode.

6. Multilayer Films Containing Cyt P450_{cam}. We used pH 5.2 for assemblies containing substrate-free cyt P450_{cam}. Films were made using both the cationic PEI and PDDA and the anionic PSS. In all cases, multilayer assembly proceeded in a linear and stable fashion, as shown by QCM results similar to those for the Mb films. Films prepared on quartz gave absorbance maxima of 397 nm, smaller than the value of 416 nm at pH 7 for substrate-free cyt P450_{cam} in solution.³²

Voltammetric peaks for the cyt P450_{cam} heme Fe(III)/Fe(II) redox couple (Figure 7) were observed in all films. Peaks were largest in assemblies with PSS. Cyt P450_{cam} has a negative charge at pH above its isoelectric point (pI)^{23b} of pH 4.6. Nevertheless, it was possible to assemble cyt P450_{cam} with both polycations and with polyanions, including DNA. It is possible that charged patches on the surface of cyt P450_{cam} permit

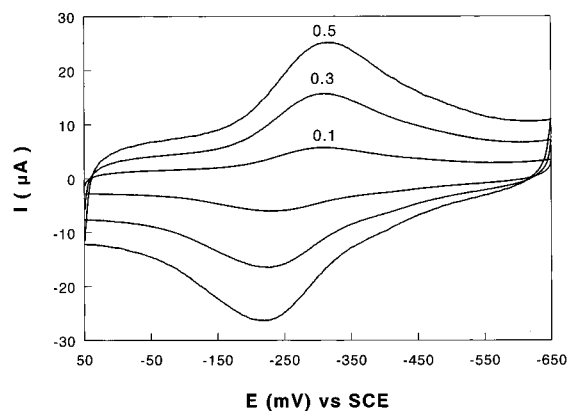


Figure 7. Cyclic voltammograms of Au + {MPS + PEI+PSS/Cyt P450_{cam}} film in TRIS buffer, pH 7, at scan rates of 0.1, 0.3, and 0.5 V s⁻¹.

Table 3. Mb/PSS (0.5 M NaCl) Multilayers Deposited on 3.8 nm Layer of {MPS + PEI/PSS (0.5 M NaCl)}^a

film composition	E° V vs NHE	CV charge $\mu\text{C cm}^{-2}$	$10^{10} \text{ mol cm}^{-2} \text{ Mb}$	
			electroactive	QCM
Mb	0.040	7.0	0.73	0.96
Mb/PSS	0.032	4.0	0.42	0.96
Mb/PSS/Mb	0.035	7.6	0.79	1.9
Mb/PSS/Mb/PSS	0.032	6.4	0.67	1.9

^a CV measurements performed at pH 5.5 in 0.1 M KCl.

interactions with both types of polyions or that non-Coulombic interactions with PSS become important at the pH used, just slightly above the pI.

To provide positive electrostatic attraction of the first cyt P450_{cam} monolayer to the electrode, we first adsorbed a bilayer of PEI/PSS onto the negative MPS-Au surface. In the next step, a layer of cyt P450 at pH 5.2 was deposited. Further alternate assembly proceeded as described above, providing cyt P450/PSS multilayers. A typical step of growth for a cyt P450/PEI multilayer measured by QCM was $-\Delta F = 80 \text{ Hz}$ for PSS and 300 Hz for enzyme, corresponding to 820 ng cm^{-2} and $0.18 \times 10^{-10} \text{ mol cm}^{-2}$ of cyt P450_{cam}.

CVs of PEI/PSS/cyt P450 films on Au-MPS were reversible in oxygen-free pH 7 buffers (Figure 7), suggesting direct electron exchange between the gold electrode and the heme Fe(III)/Fe(II) couple of the enzyme. A linear dependence of peak current on scan rate from 0.01 to 1 V s⁻¹ was found, indicating thin layer electrochemistry in the film. The midpoint potential was -0.250 V vs SCE (-0.006 V vs NHE) at pH 7 in 0.1 M NaCl.

7. Catalytic Activity for Oxidation of Styrene. The oxidation of styrene to styrene oxide can be catalyzed by both Mb and cyt P450_{cam}.³³ We recently achieved electrochemically driven styrene epoxidation using these proteins dissolved in aerobic solutions.^{24c,30b} The reaction features electrochemical reduction of oxygen catalyzed by cyt P450_{cam} or Mb. Hydrogen peroxide generated from catalytic and direct electrochemical reduction of oxygen converts a fraction of enzyme to oxidatively active forms, which transfer an oxygen atom to styrene. The main products are styrene oxide, the enzyme catalyzed product, and benzaldehyde, which results mainly from reaction of styrene with hydrogen peroxide.^{33a,b} Oxidation of styrene is thus accomplished by using the electrode as electron donor to reduce Fe^{III} and Fe^{II}-O₂ forms of the protein.

(31) Gunsalus, I. C.; Wagner, G. C. *Methods Enzymol.* **1978**, *52*, 166–188.

(32) Peterson, J. A. *Arch. Biochem. Biophys.* **1971**, *144*, 678–693.

Table 4. Results of Styrene Oxidation at 4 °C Catalyzed by Protein–Polyion Films^a

system (pH 7.4, saturated with styrene and O ₂)	amt ^b protein (nmol)	styrene oxide found (nmol)	benzald. found (nmol)	turnover no. ^c (h ⁻¹)	[H ₂ O ₂] found (mM)
Au-MPS-PEI/PSS/Mb	0.68	5.8	30	5.6	10
Au-MPS-(Mb/PSS) ₂	0.77	6.4	18	3.8	20
Mb in soln (Au)	325	50	56	0.14	5
Au-MPS-(cyt P450/PDDA) ₂	0.43	6.0	7.0	9.3	20
P450 _{cam} in soln (Au)	28	12	8	0.35	5
control (Au)	0	2.3 ^d	7.4		2
control (Au-MPS-PEI/PSS)	0	2.0 ^d	6.4		2
chemical rxn + 20 mM H ₂ O ₂	0	2.4 ^d	39		20
chemical rxn + 10 mM H ₂ O ₂	0	<0.7	26		10

Oxidation of styrene was successfully catalyzed by polyion films containing Mb or cyt P450_{cam} (Table 4). Electrolysis in the presence of oxygen using films containing Mb or cyt P450_{cam} on Au gave 3-fold more styrene oxide than controls employing electrolysis or addition of 20 mM hydrogen peroxide. The protein films gave significantly more hydrogen peroxide than the electrolysis controls, consistent with electrochemical catalysis of oxygen reduction, as found previously for these proteins in solution.^{24c,30b} We can now better understand the protein film CVs in the presence of oxygen (Figure 5), which have large peaks due to protein-catalyzed reduction of oxygen to give hydrogen peroxide.

Turnover numbers of cyt P450_{cam} were larger than those of Mb in films and in solutions, with similar ratios for cyt P450_{cam}/Mb in the two types of systems (Table 4). Enzyme activity was much higher in the films than in solution. Part of the reason for this may be the superior electron-transfer properties of the films on Au-MPS compared to the proteins in solution on bare Au.

Discussion

The alternate polyion layer-by-layer method was successfully used to make films containing Mb and cyt P450_{cam}, usually attached with oppositely charged polyelectrolytes. QCM mass monitoring confirmed that each step provided a new monolayer of adsorbate. Mb/PSS films gave stable, reversible voltammetric peaks involving the heme Fe^{III}/Fe^{II} redox couples of the proteins. The first protein monolayer in all films was fully electroactive. The second Mb layer was only partly active, and third and further layers did not increase redox activity.

The rate constant for electron transfer, k' , between electrodes and surface-localized species, can be related to electron-transfer distance d , relative to rate constant k_0 at contact distance d_0 by³⁴

$$k' = k_0 \exp[-\beta(d-d_0)]$$

The drop-off in rate with distance is rapid, with the decay constant (β) typically 8.5–11.5 nm⁻¹.

The first monolayer of Mb in our films on Au-MPS is 0.5 nm from the gold electrode. The second Mb layer is at 4 nm, and the third at 8 nm, and so on. Full electroactivity was found only for the layer closest to the electrode. It is clear, then, that distance from the electrode is a crucial parameter for electroactivity of the protein layers. The second Mb monolayer in

Au-MPS-(Mb/PSS)_x located 4 nm from the electrode provides 30–40% additional charge above Au-MPS-(Mb/PSS), which suggests an apparent $\beta < 1 \text{ nm}^{-1}$. This abnormally small β suggests that average distances between protein and Au are significantly smaller than estimated layer thicknesses. This could result from significant neighboring layer intermixing, as confirmed in *linear* polyion films by neutron reflectivity.^{12c} The high electroactivity of the single Mb monolayers placed 1.8 and 3.8 nm from the gold surface is also consistent with this view. Another explanation of redox signal increase after deposition of second protein layers is the possibility that during adsorption of the second protein layer defects in the first layer may be healed.

Laurent and Schlenoff²⁰ explored electron transfer to multiple electroactive layers of poly(butyl viologen)/PSS and found that CV peaks increased with number of viologen layers up to 10. In this case, neighboring layers of poly(butyl viologen) were interpenetrated with PSS for up to 3 bilayers. This is likely to facilitate electroactivity through the thicker film.

Bartlett et al.²² reported that the integrated charge from one poly(allylamine)ferrocene/glucose oxidase bilayer was 4.5 $\mu\text{C cm}^{-2}$, 6 $\mu\text{C cm}^{-2}$ from two bilayers, and 8 $\mu\text{C cm}^{-2}$ from three bilayers. The relative increase in charge with increasing number of layers was comparable to our results. From one to three Mb layers in our films, the charge ranged from 3 to 7 $\mu\text{C cm}^{-2}$ (Tables 1–3).

It is of interest to compare the redox activity of Mb/polyanion multilayers with cast films of Mb and insoluble surfactants, which also give reversible voltammetry.⁶ The two types of films gave surprisingly similar CV peak currents. Electroactive Mb of 0.3–0.7 $\times 10^{-10} \text{ mol cm}^{-2}$ is a typical range for both types of films. In polyion films, only the first Mb monolayer is fully active. The cast Mb-surfactant films, however, were quite dilute in Mb, containing about 1–3 mM. At pH 5.5 about half of the total Mb in the surfactant films is not electroactive.^{6f,g} Thus, the layered polyion-Mb films give similar Mb electroactivity for a monolayer and may make more efficient use of protein than in cast surfactant films.

Very little electrochemical activity for Mb in solution was found on bare, untreated vapor-deposited gold electrodes.^{6d} On bare metal and PG electrodes, macromolecular impurities are adsorbed from Mb solutions which block electron transfer between the electrode and Mb in solution. In our layer-by-layer approach, chemisorbed MPS on gold provides a uniform negative surface and adsorbed Mb at a pH where it is positively charged. The MPS layer was necessary for efficient electron transfer. We have thus employed dominating electrostatic attractions providing for Mb monolayer formation. The pro-

(33) For studies of solution enzyme catalysis of styrene epoxidation, see: (a) Ortiz de Montellano, P. R.; Fruetel, J. A.; Collins, J. R.; Camper, D. L.; Loew, G. H. *J. Am. Chem. Soc.* **1991**, *113*, 3195–3196. (b) Fruetel, J. A.; Collins, J. R.; Camper, D. L.; Loew, G. H.; Ortiz de Montellano, P. R. *J. Am. Chem. Soc.* **1992**, *114*, 6987–6993. (c) Ortiz de Montellano, P. R.; Catalano, C. E. *J. Biol. Chem.* **1985**, *260*, 9265–9271. (d) Rao, S. I.; Wilks, A.; Ortiz de Montellano, P. R. *J. Biol. Chem.* **1993**, *268*, 803–809. (e) Choe, Y. S.; Rao, S. I.; Ortiz de Montellano, P. R. *Arch. Biochem. Biophys.* **1994**, *314*, 126–131.

(34) Closs, G.; Miller, J. *Science* **1988**, *240*, 440–444. (b) Wuttke, D.; Bjerrum, M.; Winkler, J.; Gray, H. *Science* **1992**, *256*, 1007–1111. (c) Moser, C.; Keske, J.; Warncke, K.; Farid, R.; Dutton, P. *Nature* **1992**, *355*, 796–802.

Table 5. Comparisons of E° Values for Films and Solution^a

sample	E° , mV vs NHE		ref
	pH 5.5	pH 7.0	
Au-MPS-Mb	7		this work
Au-MPS-Mb/PSS	2	-90	this work
Au-MPS-PEI/PSS (0.5 M NaCl)/Mb	40		this work
Au-MPS-PEI/PSS (0.5 M NaCl)/Mb/PSS	32		this work
Au-MPS-Mb/DNA	14		this work
Mb in solution		50	35
Mb-DDAB (cast films on PG or Au)	50 (Au), 93 (PG)	1 (PG)	6d,f
Mb-DMPC (cast films on PG)	-36	-101	6f
Mb-DNA (cast films on PG)	-10	-72 (pH 7.5)	37
Mb-DHP (cast films on PG)		-89 (pH 7.4)	6e
Au-MPS-PEI/PSS/Cyt P450 _{cam}		-6	this work
substrate-free cyt P450 _{cam} in soln		-303	36
cyt P450-DMPC (cast film on PG)		-121	5
cyt P450-DDAB (cast film on PG)		22	5

^a Acronyms: PG, pyrolytic graphite; DDAB, didodecyltrimethylammonium bromide; DMPC, dimyristoylphosphatidylcholine; DHP, dihexadecylphosphate.

cedure gave similar electrochemically active films for Mb "as received" from Sigma or purified by ultrafiltration. This suggests that impurities in the Mb solutions do not compete well with electrostatically driven Mb adsorption.

Formal potentials of Mb in the films are controlled by the pH of the external solution. The shift of -55 mV pH^{-1} suggests a single protonation accompanying electron transfer. A similar proton-coupled electron transfer was identified in cast films of Mb and DMPC or DDAB.^{6f}

Formal potentials for the proteins in the films are not the same as for the respective protein dissolved in solution. Compared to solution values, formal potentials are shifted negative for Mb and positive for cyt P450_{cam}. Similar trends concerning E° were found for Mb and cyt P450_{cam} in cast films of lipids and surfactants and depended on surfactant headgroup charge (Table 5).^{5,6b,e,f}

The surface charges of Mb and cyt P450_{cam} are very different. At pH 5–7, Mb is positive (pI 7.5), while cyt P450_{cam} is negative (pI 4.6). This provides a clue that formal potentials in the films may be governed by electrostatic interactions. These may include both protein–polyion interactions and electrode double layer effects on the potential felt by the protein and may be similar in polyion and surfactant films.^{6b} Another factor to consider is partial unfolding of the protein structures. Soret band positions do not support full unfolding and loss of heme, however, which would also be expected to result in unstable voltammetry, as discussed earlier. Spin state also influences both formal potential and Soret band position of Fe^{III} heme proteins.^{35,36,38} A spin state change is inconsistent with the Mb film spectrum.³⁸ However, the cyt P450_{cam} Soret band at 397

nm in the films, shifted from 416 nm for the low spin form, could result from a change to high spin Fe(III) similar to that found upon binding the substrate camphor.³² Clearly, further studies are needed to elucidate protein secondary structure in these films.

Despite the different Soret band positions compared to solutions, both Mb and cyt P450_{cam} in polyion films had good catalytic activity for styrene epoxidation (Table 4). This shows that the proteins retain enzyme-like catalytic properties in the films. In fact, turnover numbers suggest that enzyme activity in the films was significantly better than in solution.

Conclusions

Stable, ordered, multilayer films containing electrochemically and catalytically active myoglobin and cyt P450_{cam} in alternation with polyanions were prepared on MPS–Au electrodes. Direct, reversible electron transfer between electrodes and proteins involved the heme Fe^{III}/Fe^{II} redox couple. In the presence of oxygen, electrons were transferred to the Fe^{II}–O₂ complexes of these proteins to yield hydrogen peroxide. Accomplishment of these electron transfers allowed the films to be used for electrode-driven enzyme-like catalysis, which was demonstrated for epoxidation of styrene.

Acknowledgment. This publication was supported by U.S. PHS Grant No. ES03154 from the National Institute of Environmental Health Sciences (NIEHS), NIH. Its contents are solely the responsibility of the authors and do not necessarily represent the official views of NIEHS, NIH.

Supporting Information Available: Complete experimental details and four figures (9 pages, print/PDF). See any current masthead page for ordering information and Web access instructions.

JA9737984

(35) King, B. C.; Hawkrige, F. M.; Hoffman, B. M. *J. Am. Chem. Soc.* **1992**, *114*, 10603–10608.

(36) Sligar, S. G.; Cinti, D. L.; Gibson, G. G.; Schenkman, J. B. *Biochem. Biophys. Res. Commun.* **1979**, *90*, 925–932.

(37) Nassar, A.-E. F.; Rusling, J. F.; Nakashima, N. *J. Am. Chem. Soc.* **1996**, *118*, 3043–3044.

(38) Eaton, W. A.; Hochstrasser, R. M. *J. Chem. Phys.* **1968**, *49*, 985–995.